

## **Electronic Supplementary Information**

### **Morphological Conversion of Dipolar Core-Shell Au-Co Nanoparticles into Beaded Au-Co<sub>3</sub>O<sub>4</sub> Nanowires**

*Bo Yun Kim,<sup>a</sup> Seung-Ho Yu,<sup>b</sup> Hyun Sik Kim,<sup>a,b</sup> Dong-Chan Lee,<sup>b</sup> In-Bo Shim,<sup>c</sup> Sean E. Derosa,<sup>a</sup> Yung-Eun Sung,<sup>b</sup> and Jeffrey Pyun<sup>a,b\*</sup>*

<sup>a</sup>Department of Chemistry, University of Arizona, 1306 E. University Blvd. Tucson, AZ 85752, <sup>b</sup>World Class University Program for Chemical Convergence for Energy & Environment, Department of Chemical & Biological Engineering, Seoul National University, Seoul 151-744, Korea, <sup>c</sup>Department of Nano and Electronic Physics, Kookmin University, Seoul, Korea, 136-702,

Email: [jpyun@email.arizona.edu](mailto:jpyun@email.arizona.edu)

#### **EXPERIMENTAL**

**Materials and Characterization.** Anhydrous 1,2-dichlorobenzene (DCB), toluene (99.5%), 1,2,3,4-tetrahydronaphthalene (tetralin, 99%), oleylamine (70%), NaOH (99.99%) and gold(III) chloride trihydrate (HAuCl<sub>4</sub>·3H<sub>2</sub>O 99.9%) were purchased from Aldrich. Dicobalt octacarbonyl (Co<sub>2</sub>(CO)<sub>8</sub>, Strem) and absolute ethanol (Pharmco-Aaper) were commercially available. All commercially obtained reagents were used as received without further purification. An Omega temperature controller CSC32K with a K-type utility thermocouple and a Glas-Col fabric heating mantle were used for

thermolysis reactions. Calcinations of PS-AuCo core-shell nanoparticles were performed either in the Barnstead/Thermolyne small bench-top muffled furnace in an air or in the Lindberg Sola Basic tube furnace (model: M-1018-vs) with Staco Energy variable autotransformer under Ar. TEM images were obtained on a Phillips CM12 transmission electron microscope (CM12) either at 80 kV or at 100 kV, using in house prepared carbon coated copper grids (Cu, hexagon, 300 mesh) and carbon coated nickel grids (Ni, hexagon, 300 mesh). Image analysis was performed using ImageJ software (Rasband, W.S., National Institutes of Health, <http://rsb.info.nih.gov/ij/>, 1997-2007). Relative uncertainty of particle size determinations using ImageJ was found to be 1 % of diameter average (e.g.,  $20 \pm 0.2$  nm). SEM images were taken on a Hitachi 4800 FE-SEM on the as-prepared samples (i.e., no metallic over coating).

**Preparation of gold nanoparticles (AuNPs).** Gold nanoparticles were synthesized by method reported in the literature.<sup>1</sup> HAuCl<sub>4</sub>·3H<sub>2</sub>O (0.500 g, 1.25mmol) was added to 50 mL of tetralin, followed by an addition of oleylamine (5.00 ml, 15.0 mmol) to form a dark red solution. The solution was heated at 65 °C for 5 hours and then cooled to room temperature. Gold nanoparticles were precipitated by adding ethanol and isolated by centrifugation (yield = 0.237 mg). Sample for TEM analysis was prepared by dispersing the isolated Au NP powder in toluene (1 mg/2 mL) via sonication for 15 minutes, followed by drop casting onto a carbon coated Cu grid. The particle size of resulting Au nanoparticles measured by TEM was  $13 \pm 3$  nm.

**Preparation of PS-AuCoNPs, using amine end-functionalized polystyrene ligands (PS-NH<sub>2</sub>)** PS-AuCoNPs was synthesized according to our previous report.<sup>1</sup> PS-NH<sub>2</sub> (0.100 g;  $1.42 \times 10^{-2}$  mmol;  $M_n = 7000$  g/mol;  $M_w/M_n = 1.07$ ) and Au NPs (0.100 g)

were dissolved in 10 mL and 5 mL of DCB, respectively. These two solutions were transferred into a three-neck round bottom flask containing DCB (5 mL) and the resulting mixture was heated to reflux at 175 °C. Separately,  $\text{Co}_2(\text{CO})_8$  (0.400 g;  $1.16 \times 10^{-3}$  mol) was dissolved in DCB (4 mL) at room temperature in air and was rapidly injected into the hot Au and polymer solution. Upon the injection, the reaction temperature dropped to around 155 °C and maintained at 160 °C for 60 minutes, followed by cooling to room temperature under argon. PS-Au-Co core-shell NPs were isolated by precipitation into hexanes (500 mL), yielding a black powder (yield = 0.317 g) soluble in a wide range of non-polar solvents (e.g., methylene chloride, THF, and toluene). Sample for TEM analysis was prepared by dispersing the isolated powder in toluene (1 mg/2 mL) via sonication for 15 minutes followed by drop casting onto a carbon coated Cu grid.

**Calcination of PS-AuCoNPs** PS-AuCoNPs dispersion in toluene (1 mg/ml) was either spin cast or drop cast on Si wafers then calcined at 400 °C, 500 °C, and 600 °C in the furnace under Ar and air to yield AuCo and  $\text{AuCo}_3\text{O}_4$  heterostructures nanowires, respectively. The tube furnace was purged with Ar and stabilized at desired temperature for an hour prior to use. For TEM imaging, PS-AuCoNPs on Ni grids (300 meshes) was calcined under same condition.

## 2. Kinetic Study of Morphological Transformation of PS-AuCoNPs

Kinetic study of morphological transformation demonstrated to optimize annealing condition for preparation of heterodimer structured nanowires. PS-AuCoNPs dispersion solution in toluene was drop cast on Si wafers and calcined at 500 °C, 600 °C, and 700 °C for various times. Morphological transformation of PS-AuCoNPs upon annealing under different temperatures was monitored by FE-SEM. The core-shell morphology of PS-AuCoNPs was intact in  $\text{AuCo}_3\text{O}_4$  NWs annealed at 500 °C for 4 hrs (Figure S1a). After 8h calcination at 500 °C, cobalt oxide nanowires revealed rough surfaces however gold cores were remained inside of nanowires (Figure S1b). After 12h calcination at 500 °C (Figure S1c), partially exposed gold cores were observed and eventually gold core migrated out from interior to exterior of cobalt oxide shell after calcination for 18 hrs (Figure S1d).

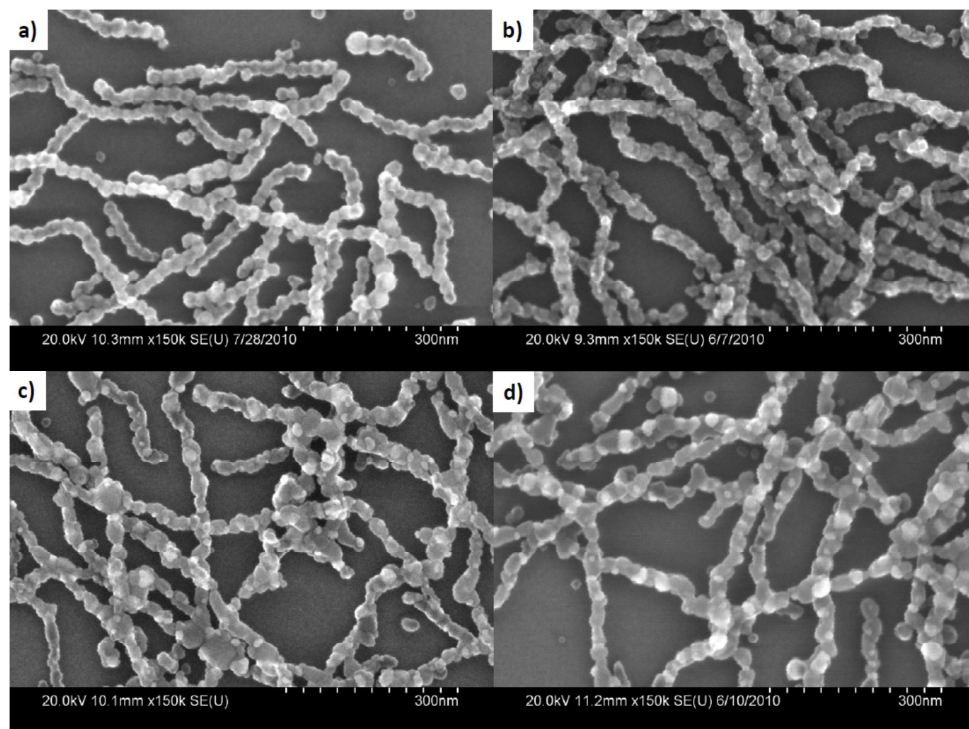


**Figure S1.** FESEM images of PS-AuCoNPs on a Si substrate after calcination at 500 °C for (a) 4 hrs, (b) 8 hrs, (c) 12 hrs, and (d) 18 hrs in the air

Figure S2 showed AuCo<sub>3</sub>O<sub>4</sub> nanowires annealed at 600 for 3 and 6 hrs and at 700 °C for 1 hr. The migration of Au cores toward the exterior of cobalt oxide shells started to occur after calcination at 600 °C for 1hr and completed after annealing at 600 °C for 3hr, forming a heterodimer type morphology as shown in Figure S2b. Calcination at 600 °C for 6 hrs caused fragmentation of cobalt oxide shell and SEM image exhibited Au placement in between Co<sub>3</sub>O<sub>4</sub> fragments to form “segmented nanowires” (Figure S2c). Annealing at even higher temperature (700 °C) accelerated the conversion process, resulting in segmentation of cobalt oxide nanowires after 1 hr (Figure S2d).

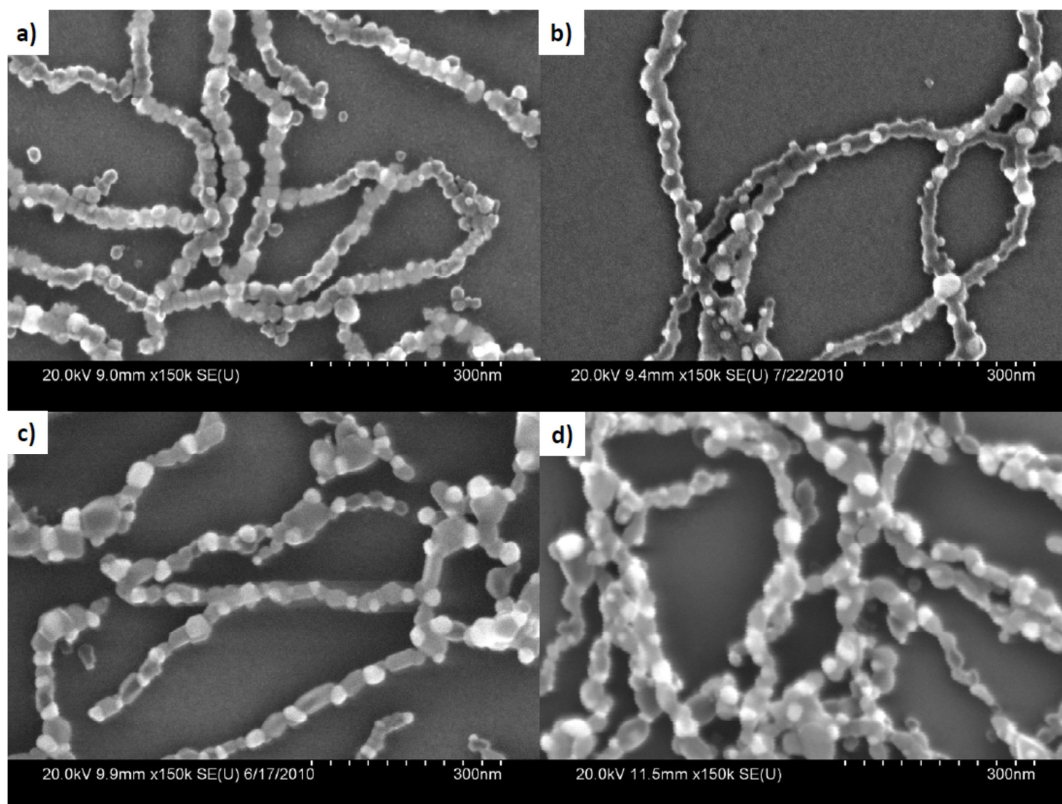


**Figure S2.** FESEM images of PS-AuCoNPs on a Si substrate after calcination for (a) 1 hr, (b) 3 hrs, (c) 6 hrs at 600°C and (d) 1 hrs at 700°C in the air

### 3. XRD of calcined AuCo<sub>3</sub>O<sub>4</sub> NWs

Powder X-ray diffraction (XRD) was used to characterize the solid-state structure of Au-Co<sub>3</sub>O<sub>4</sub> nanowires calcined at different temperature. Calcination of PS-AuCo NPs at 400, 500, and 600 °C removed the organic PS outer shells and yielded polycrystalline Co<sub>3</sub>O<sub>4</sub> (Fig. S3). For Au-Co<sub>3</sub>O<sub>4</sub> nanowires calcined and annealed at 400 °C the diffraction patterns were dominated from AuNP inclusions due to both the higher Z of Au relative to Co atoms and the significant weight fraction of Au present in the material. However, diffraction peak corresponding to the spinel Co<sub>3</sub>O<sub>4</sub> phase were also observed.<sup>2</sup> Calcination at 500, and 600 °C indicated that both spinel Co<sub>3</sub>O<sub>4</sub> and metallic Au were present, although a sharpening and amplification of diffraction peaks for spinel Co<sub>3</sub>O<sub>4</sub> was observed for peaks in region of 37 and 67 degrees 2-theta. We attributed this enhancement to the crystallization of Co<sub>3</sub>O<sub>4</sub> phases as a consequence of both the high temperature annealing step and the morphological conversion from core-shell to beaded nanowires, as previously discussed.

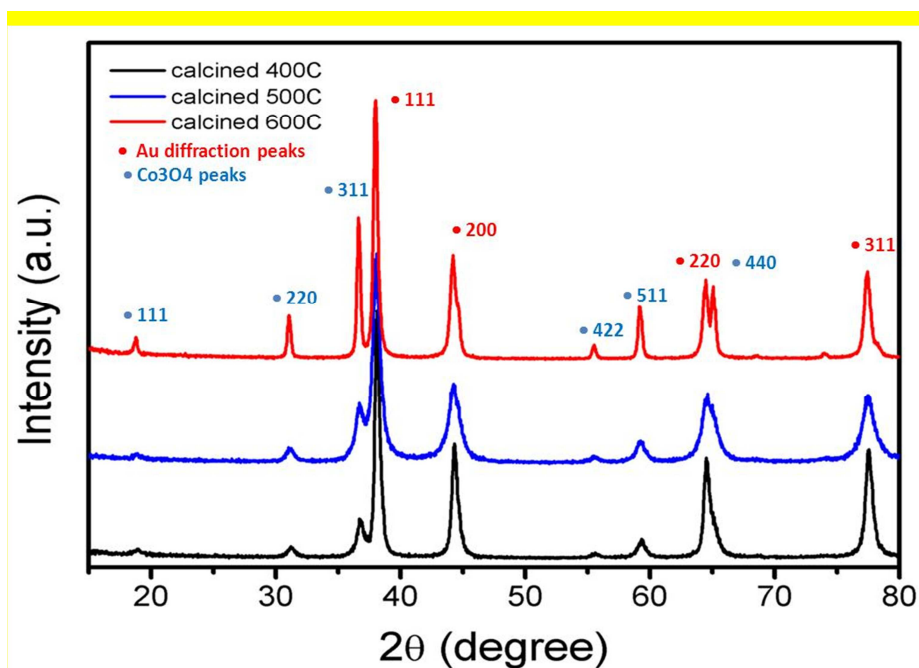


**Figure S3.** XRD of calcined PS-AuCoNPs at 400°C (bottom black line), 500°C (middle blue line), 600°C (top red line) in air for 10hrs

**Fabrication and evaluation of positive electrodes using Au-Co<sub>3</sub>O<sub>4</sub> powders for Li-Batteries.** Working electrodes were prepared from a formulation of Au-Co<sub>3</sub>O<sub>4</sub> powder, Super P (as a conducting agent) and polyvinylidene fluoride (PVDF, as a binder) (75: 10:15 in weight ratio) in n-methyl-2-pyrrolidinone (NMP) solvents. The slurry was coated onto a copper foil current collector via doctor blade processing and then pressed for use as the working electrode. Electrochemical test cells were assembled in an argon-filled glove box using coin-type half-cells (2016 type) with lithium foil as a counter electrode. The organic electrolyte was composed of 1.0 M LiPF<sub>6</sub> in ethylene carbonate (EC) and diethyl carbonate (DEC) (1:1 vol.%) The cells were galvanostatically charged and discharged in the voltage range from 3.0 to 0.01 V vs. Li/Li<sup>+</sup> at a current density of 100 mA/g. Electrochemical measurements were made with a WBCS3000 cycler (WonA Tech, Korea) at room temperature.

In the initial evaluation of calcined Au-Co<sub>3</sub>O<sub>4</sub> nanowire powders in half-cell coin-type cells for Li-insertion experiments, high capacities around 600-700 (mAh/g) were observed out to 30 cycles. However, when experiments were continued out to 50 cycles, significant fading of capacity was observed (300 mAh/g), indicating that Au-Co<sub>3</sub>O<sub>4</sub> did not exhibit robust electrochemical behavior (Fig. S4). To further confirm this observation, additional control experiments with hollow Co<sub>3</sub>O<sub>4</sub> nanowire powders<sup>3</sup>



of similar size were investigated, along with simple blends (with identical wt% of Au and Co as for the Au-Co<sub>3</sub>O<sub>4</sub> electrodes) of oleylamine coated AuNPs<sup>4</sup> ( $D = 10 \text{ nm} \pm 2$ ) and hollow Co<sub>3</sub>O<sub>4</sub> nanowires that were homogeneous in solution, and processed using identical conditions for Au-Co<sub>3</sub>O<sub>4</sub> materials before battery evaluation (Fig. S5). Surprisingly, electrodes fabricated from hollow Co<sub>3</sub>O<sub>4</sub> nanowires exhibited the highest and most electrochemical stability specific capacity out to 50 cycles (800-1000 mAh/g). Li-insertion experiments with electrode fabricated from blends of AuNPs and Co<sub>3</sub>O<sub>4</sub> nanowires exhibited initially lower specific capacity values (500-600 mAh/g), but exhibited significantly more stable cycling behavior and retention of capacity than the heterostructured Au-Co<sub>3</sub>O<sub>4</sub> electrodes.

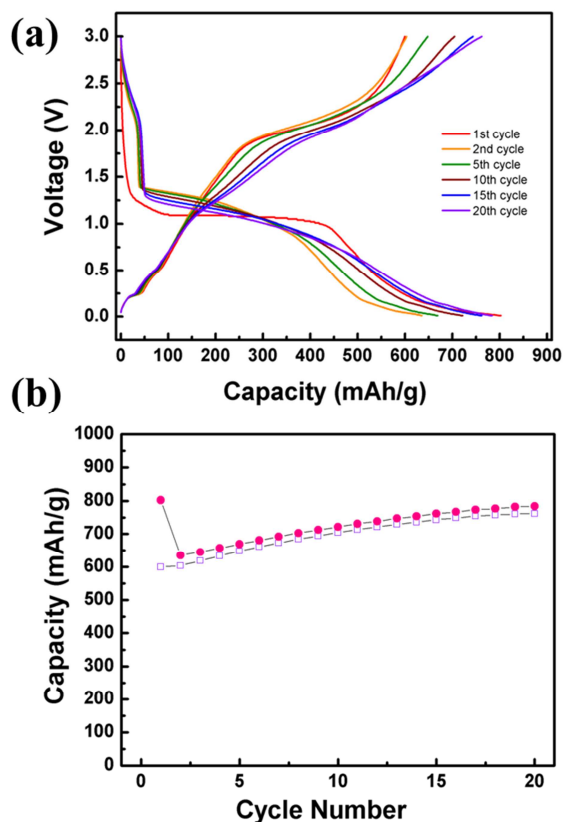


**Figure S4:** specific capacity-cycle number profiles of Au-Co<sub>3</sub>O<sub>4</sub> negative electrodes for charge (closed circles) and discharge (open circles),



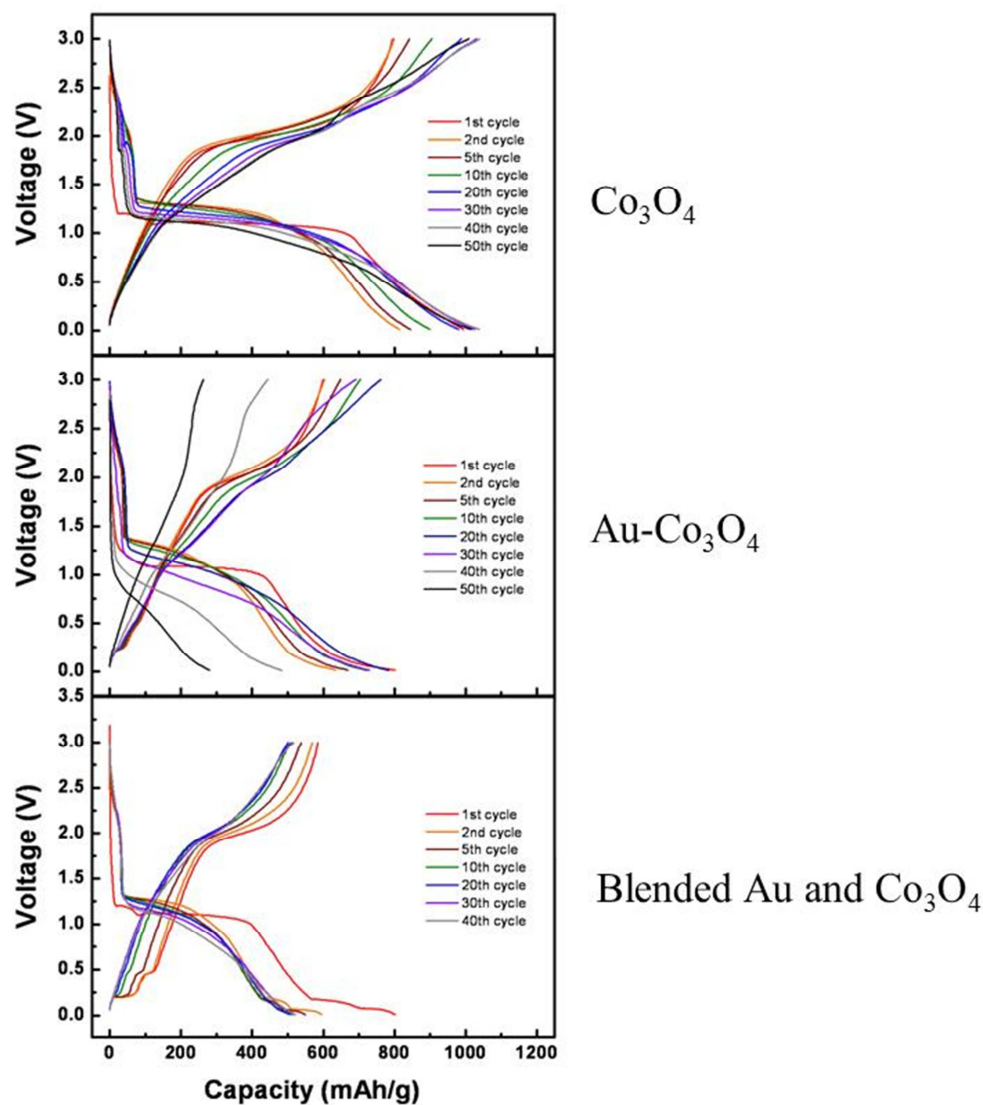


**Figure S5:** Voltage-capacity profiles of electrodes fabricated and measured against Li electrodes from  $\text{Co}_3\text{O}_4$ ,  $\text{Au-Co}_3\text{O}_4$  and blends of AuNP and  $\text{Co}_3\text{O}_4$  nanowires.

## References

1. Kim, B. Y.; Shim, I.-B.; Araci, Z. O.; Saavedra, S. S.; Monti, O. L. A.; Armstrong, N. R.; Sahoo, R.; Srivastava, D. N.; Pyun, J. *J. Am. Chem. Soc.* **2010**, *132*, 3234-3235.

2. He *et al.*, *Chem. Mater.*, **2005**, *17* (15), 4023-4030
3. Keng, P.; Kim, B.; Shim, I.-B.; Sahoo, R.; Veneman, P.E.; Armstrong, N.R.; Yoo, H.; Permberton, J.E.; Bull, M.M.; Griebel, J.J.; Ratcliff, E.L.; Nebesny, K. G.; Pyun, J. *ACS Nano* **2009**, *10*, 3143-3157.
4. Kim, B.; Shim, I.-B.; Monti, O.A.; Pyun, J. *Chem. Commun.* **2011**, *47*, 890-892.